

Skin cancer classifier based on convolution residual neural network

Ahmed R. Ajel¹, Ayad Qasim Al-Dujaili¹, Zaid G. Hadi¹, Amjad Jaleel Humaidi²

¹Department of Medical Instrumentation, Middle Technical University, Electrical Engineering Technical College, Baghdad, Iraq

²Control and Systems Engineering Department, University of Technology, Baghdad, Iraq

Article Info

Article history:

Received Aug 20, 2021

Revised May 10, 2022

Accepted May 11, 2022

Keywords:

Convolution neural networks

Deep learning

Deep learning convolutional neural network

Melanoma classification

Skin cancer

ABSTRACT

Accurate automatic classification of skin lesion images is a great challenge as the image features are very close in these images. Convolution neural networks (CNN) promise to provide a potential classifier for skin lesions. This work will present dermatologist-level classification of skin cancer by using residual network (ResNet-50) as a deep learning convolutional neural network (DLCNN) that maps images to class labels. It presents a classifier with a single CNN to automatically recognize benign and malignant skin images. The network inputs are only disease labels and image pixels. About 320 clinical images of the different diseases have been used to train CNN. The model performance has been tested with untrained images from the two labels. This model identifies the most common skin cancers and can be updated with a new unlimited number of images. The DLCNN trained by the ResNet-50 model showed good classification of the benign and malignant skin categories. The ResNet-50 as a DLCNN has verified a significant recognition rate of more than 97% on the testing images, which proves that the benign and malignant lesion skin images are properly classified.

This is an open access article under the [CC BY-SA](https://creativecommons.org/licenses/by-sa/4.0/) license.



Corresponding Author:

Ahmed R. Ajel

Department of Medical Instrumentation, Middle Technical University, Electrical Engineering Technical College

Baghdad, Iraq

Email: dr_ahmed.r@mtu.edu.iq

1. INTRODUCTION

It is reported that there are 5.4 million new cases of skin cancer in the US alone and despite melanoma patients are less than 5%, it accounts for approximately 75% of all types of skin cancer in the US that related cause over 10,000 deaths per year [1], [2]. Melanoma is approximately 10 times more likely to spread and disseminate than all the other types of skin cancer, it is also very capricious and unpredictable most of the other types of skin cancers. It usually expects to see them in areas that are sun-exposed dominant or occupationally some exposed dominant melanoma on the other hand very unpredictable. It is seen around people's feet even in people's eyeballs are very unpredictable. The other problem with it is like an octopus it tends to borrow, and it has tentacles that tend to spread out quickly. Early detection of these cases is critical, where the 5-years survival rate drops from over 99% to 14% if detected in its latest stages [3]. According to [4]–[6], it is possible to classify human skin disease taxonomy, where red refers to malignant, orange denotes non-neoplastic, black for melanoma, and green refers to benign, as shown in Figure 1.

This classification figure has been prearranged visually and clinically with the help of medical specialists. Deep learning convolutional neural networks (DLCNN) skin image classifier enables to embed a dermatologist level classifier into our phone or personal computer (PC) by just snap a picture of user skin lesion and instantly getting such diagnosis [3]. A popular way of classifying images is that most images take

as input and by using a series of compositional filters and other miscellaneous things the deep learning communities come up with for better vision applications, and then match the images into class labels such as scattered off. The use of deep learning with an automated dermatology classifier will provide a new disease-partitioning algorithm for skin disease taxonomy that maps each disease according to training classes. The idea in this work is to detect skin cancer in clinical images by using a skin cancer classifier based on a convolution residual neural network. The considered data set in the paper consists of 320 clinical images including 160 benign and malignant classes. The skin lesion images have been resized to match the input of the DLCNN classification network. Residual network, which is called ResNet-50, as a DLCNN, is considered in this paper. ResNet-50 is a pre-trained architecture that is already trained on a database subset of the Image-Net for large-scale visual image recognition. A million images have been trained on ResNet-50, which has 177 layers corresponding to 50-layer residual networks. It can classify 1,000 images into object classes.

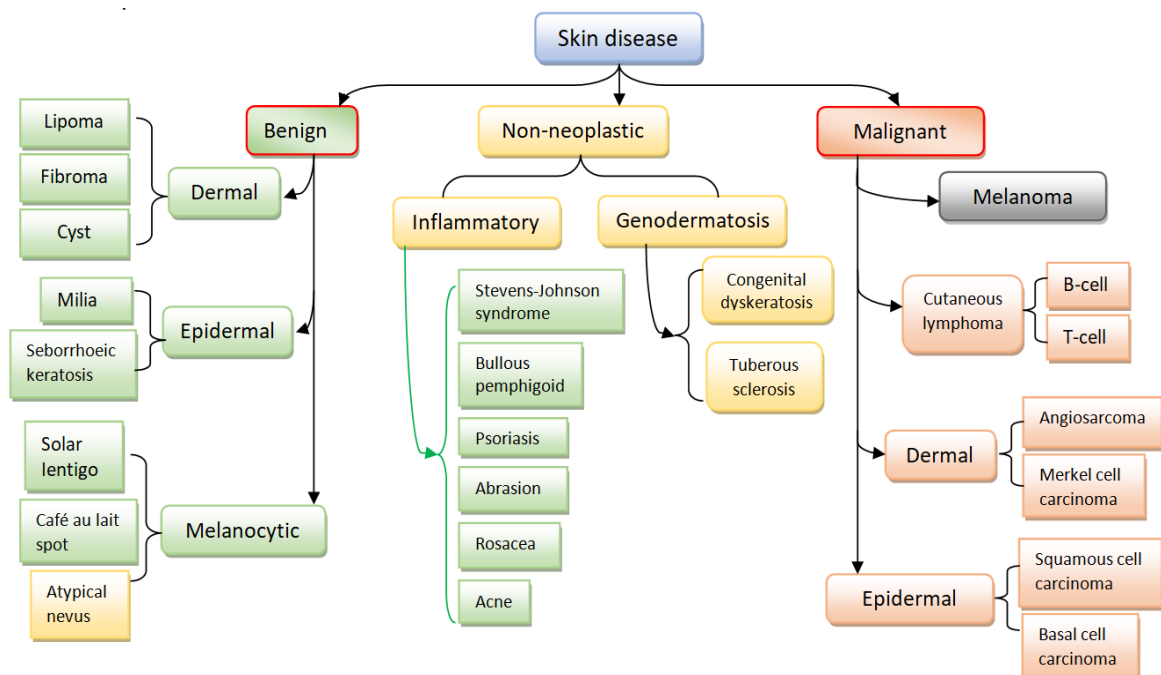


Figure 1. A diagram illustration of human skin disease taxonomy, where it is organized according to the clinical and visual similarity of the skin diseases [4]–[6]

Several deep learning techniques have been introduced to improve structure performance in solving different image processing and engineering problems. The learning techniques of DLCNN have undergone a large growth, which sharply improves its performance in various applications such as medical image classifiers [7], [8]. Several studies related to dermatological classifier [9]–[11] but they have lacked to generalize the capability of disease-partitioning with unsatisfactory information and a spotlight on standard tasks like histological [12] and dermoscopy image classifier [13]. Histological images are obtained by invasive microscopy and biopsy, while dermoscopy images are obtained by a specific device, and both modalities create consistent images. Smartphone images as photographic images show inconsistency in features such as lighting, zoom, and angle, which makes a classifier significantly further challenging [14], [15]. Other previous related studies require extraction of visual features, lesion segmentation, and extensive processing, and pre-training before classification. In this work, a data-driven approach [16], [17] is considered to overcome these challenges. Hundreds of images with photographic variability are trained to ensure robust classification. In addition, no hand-crafted features are required in our system. The presented model trains the image raw pixels and labels by a single structure for dermoscopy and photographic images. This study presents a generalized classification approach with a flexible number of input clinical datasets that reach hundreds of thousands to generalize the application over extensive dermoscopy and photography images.

Advances in DLCNN with large-scale datasets [18] that recently create different visual tasks systems of human performances, for example; playing Atari game [19], [20], object recognition [21], [22],

and strategic games such as Go [23]. Hagerty *et al.* [24] used a utilized residual network algorithm called ResNet-50 as a DLCNN for image processing to fuse the features from individual methods by hypothesizing different error profiles and using three hand-crafted biological modules for predicting the probability of melanoma categorization. However, the adopted handcraft features-based method is not clear. In this work, an image-based classification using the CNN system is developed to match dermatologists satisfactory in some significant key diagnostic aspects such as melanoma/nonmelanoma classification by means of carcinoma and dermoscopy classifications. An open-source dataset have been pre-trained over approximately 1.3 million clinical images with large-scale object categories [25], and the dataset is trained using Renet50 learning architecture [26].

2. METHOD

2.1. Diagnosis

The convolutional neural networks (CNN) are trained with skin disease classes. Our dataset is organized with dermatologist-labeled clinical images that are coming from an online open-access clinical source. We divide the dataset into 70% for training images and validations, while 30% for testing images. An algorithm, that portioning skin diseases such as melanoma and non-melanoma, is developed as a fine training class. Initially, skin lesion images are separated from adjoining artifacts and normal skin tissue like hairs, air bubbles, and veils, with mean thresholding, color space transformation, and removal of the region of interest (ROI). Then, the region of interest image employing the binary mask image a set of features based on texture, shape, and color, is obtained. The features of deep learning neural network (DLNN) are acquired appropriate CNN structure that is trained in a MATLAB-function called ResNet-50 classification algorithm that includes CNN architecture to extract image features [27]. The obtained classification is trained on a dataset consisting of both benign and malignant skin-lesion images.

2.2. Resnet-50 architecture

The deep learning (DL) part of our approach depends on a transfer learning described in [27], and a deep residual network called (ResNet), which is a convolution-based architecture [28]. Its input matrix can accept 224×224 red-green-blue (RGB) images. DL ResNet architecture is effective in a large-scale image visual recognition to classify 1,000 objects [29]–[32]. ResNet can achieve a correct recognition error of 3.6%. ResNet is a convolution-based architecture. Bicubic interpolation is usually used to reduce the resolution. A sequential series of residual blocks as shown in Figure 2 is the main property of ResNet, which results in 2,048 feature vectors.

Since this work considers the residual network as a DLCNN to solve accurately the clinical skin lesion image recognition problem, the underlying architecture is illustrated layer by layer, starting from an RGB image to an output production, including convolutional layers, batch normalization layer, and max-pooling layers. There are too many convolution layers attached one by one, and there are many skip connections called residual neural networks. A main conceptual block diagram of the proposed approach is demonstrated in Figures 3, 4, and 5. To make the structure simpler to understand, the complete architecture is broken down into 19 small blocks. The first block is shown in Figures 3(a) to 3(c).

It is known that transfer learned models have a predefined shape, which is in the start described by $1 \times 3 \times 224 \times 224$. The first one shows the batch size, then the number of RGB channels, then 224×224 are width and height of an input image. ResNet-50 is applying 64 convolutions of 7×7 kernel size and a padding of 3 and strides of 2 that represent the tensor operation. The size of the image after padding is the same as width but when applying the kernel impact the size will be reduced to 230 after padding. The output from this first convolutional layer is 64 and the output size will be $1 \times 112 \times 112 \times 64$. The batch normalization applies to a simple layer and there are 64 mean variance beta and lambda which is the scaling factor that does not make any changes with the tensor other than normalizing. In the second block, the max-pooling is applied, which has strides 2, padding 1, and the kernel size 3×3 . This is shown in Figure 4.

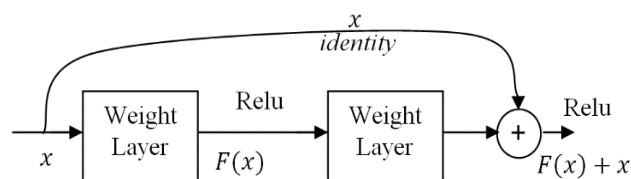


Figure 2. Residual block of ResNet-50 [28]

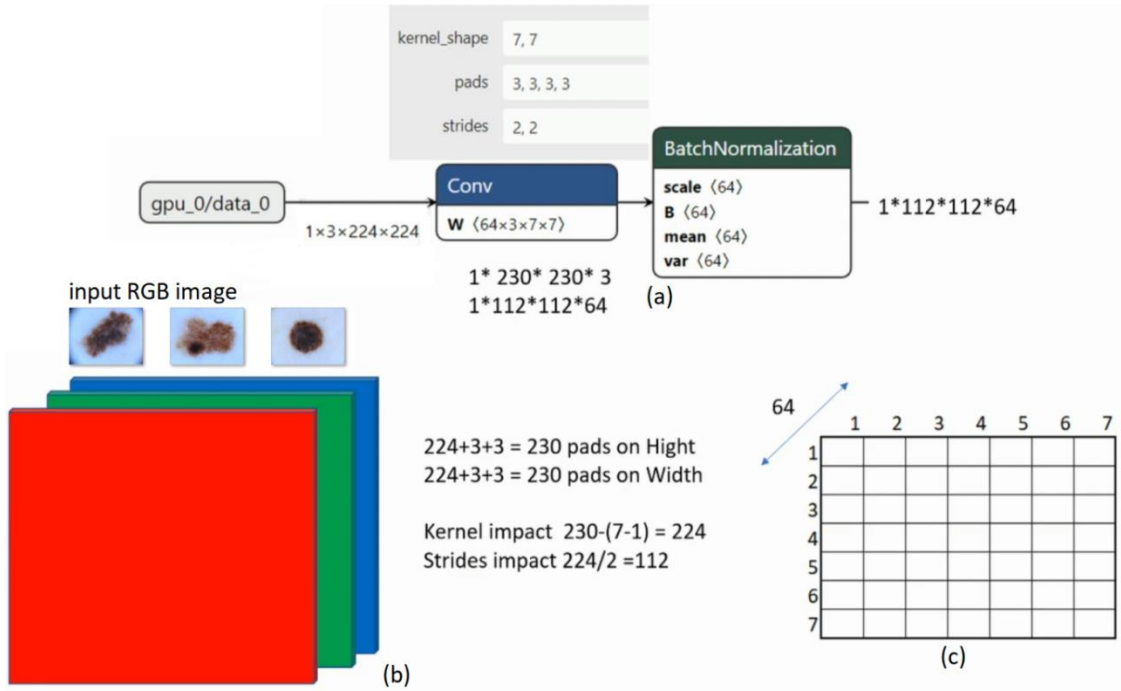


Figure 3. Block 1 of 19 ResNet-50 architecture, where (a) represents the 1st convolution operation, (b) the RGB input image, and (c) 7×7 kernel shape

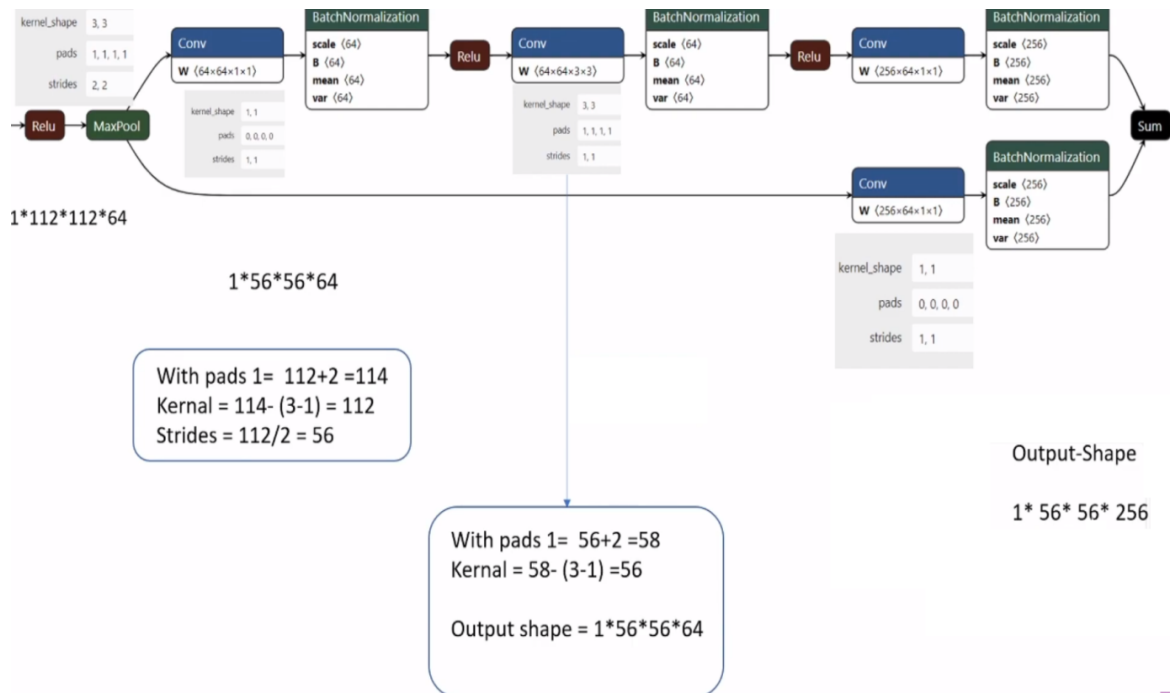


Figure 4. Block 2 of 19 of the ResNet-50 architecture

Therefore, the size is reduced and the complete shape is divided by 2 and the output shape will be $1 \times 56 \times 56 \times 64$. In this block, we have multiple convolutions on one side, then pass normalization, and the input dimension will remain the same. Another one convolution, which has the same kernel 1×1 padding, and strides are also 1×1 that makes no changes with the shape. There is a parallel connection with the simple shape of $256 \times 64 \times 1 \times 1$ that provides output $1 \times 56 \times 56 \times 256$. Therefore, only 64 got converted to 256.

Going forward in the CNN, these blocks are similar in nature actually, they are just tacked up one by one. The last end of this chain is having 256 filters in one convolution. So, it will again change the shape to 256 and this skip connection, which has been taken from this value (denoted by Relu), which is directly connecting to the sum. Getting understood of block 2 and block 3 all rest of the blocks are similar in nature. The last block of the ResNet-50 architecture is shown in Figure 5.

The last layer or block 19 includes applying an average pooling of 7×7. The average pooling is a little bit different though converting the 7×7 to 1×1 within one channel of 7×7. The output will be 1×2,048. Then a general matrix multiplication that is inclusive of softmax here. The output of the softmax is 1,000 classes and the input to the softmax is 2,048. Therefore, using this complete ResNet-50 CNN, this last softmax layer can be replaced by a defined number of classes and keeping all previous layers not trainable.

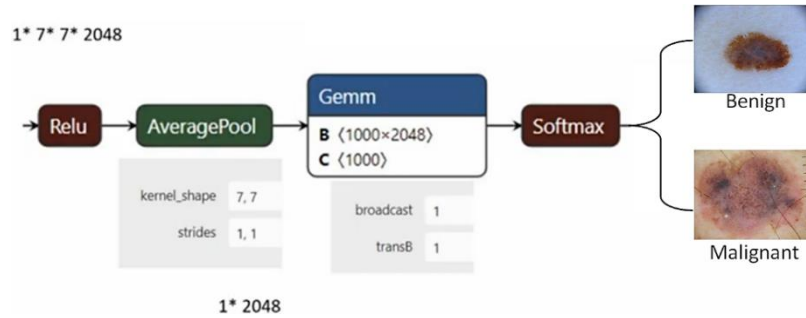


Figure 5. The 19th (final block) of 19 of the ResNet-50 architecture

3. RESULTS

The feasibility of the developed DLCNN to categorize the skin lesion images is verified by training 70% of the dataset and testing the remaining images that are not identified by the network. All patches of the residual CNN (ResNet-50) were ($n=1,687$), trained, and augmented in the training cohort in ResNet-50 to enlarge the robustness of the architecture. The upper graph of Figure 6 demonstrates the accuracy during the learning, which was found to be 0.9779, while the cross-entropy loss was close to 0.132 after 8th epochs training (248 iterations), which can be seen at the bottom of the figure. The elapsed time here was 1 min 0 seconds as the hardware resource is a single central processing unit (CPU) and not graphics processing unit (GPU). The details are also shown in Figure 6.

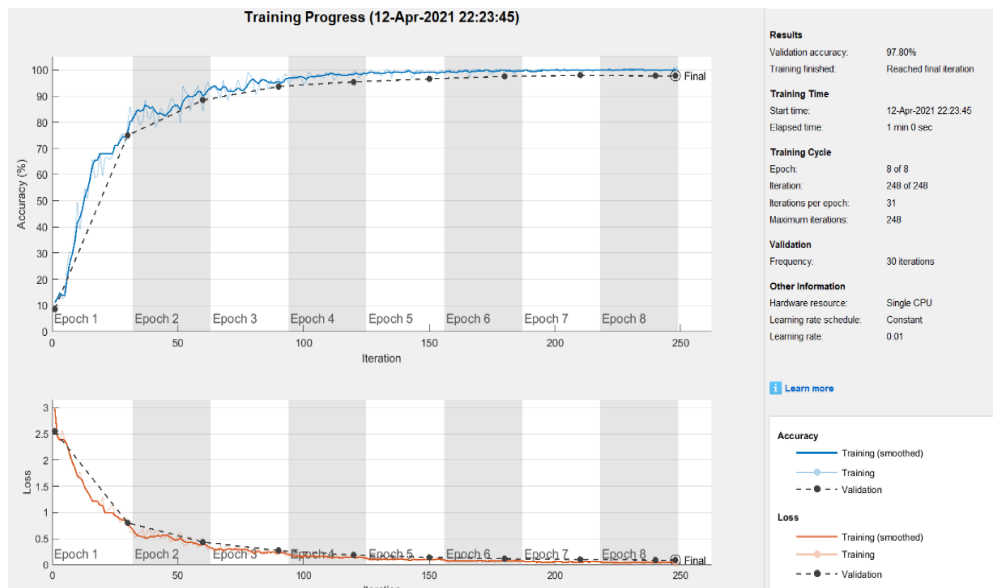


Figure 6. The process of training and validation of the DLCNN using ResNet-50 model when training skin lesion images

The accuracy is in the upper while the cross-entropy loss is in the bottom. Two categories have been classified over 248 maximum iterations. The input image is responded to or activated by each layer of the DLCNN. Some of these layers are performing the extraction of image features. The basic image features such as edges and blobs are captured by DLCNN at the beginning layers of the network. To take visual insight for the network filter weights, Figure 7 shows weights samples at the 1st convolution layer.

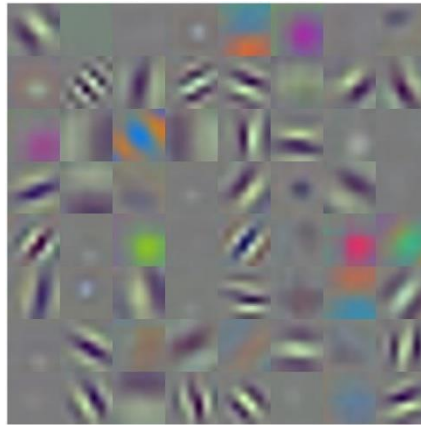


Figure 7. First convolutional layer weights

The DLCNN trained by the ResNet-50 model showed good classification of the benign and malignant skin categories. The ResNet-50 in DLCNN verified a significant recognition rate of more than 97% on the testing images, which proves that the benign and malignant lesion skin images are properly classified. Now, the predictive accuracy of DLCNN architecture can be obtained in each patch by a confusion matrix, which is displayed in Figure 8.

This study can be extended for future work by suggesting other models of deep learning or other diseases [33]–[40]. In addition, one can enhance the present research by designing embedded systems based on field-programmable gate array (FPGA) to implement the classifier within real-time environment [41]–[52].

Benign	47	1	
Malignant	4	44	
	Benign	Malignant	97.80%

Figure 8. Confusion matrix

4. CONCLUSION

This paper presents a developed residual network as a deep learning CNN for image recognition purposes to classify the lesion skin images into benign and malignant images. About 320 clinical images of the different diseases have been used to train CNN. Deep ResNet-50 network with skip connections was employed as an approach to perform the partitioning images task, which results in higher classification performance. The results of training and the verification by the testing images show that ResNet-50 DLCNN is efficiently able to accurately generalize the grade of benign and malignant images with a very small margin of error. The significance and robustness of this model in grading skin lesion images are because of its control of learning high and low levels to extract image features utilizing its deep residual networks, pooling layers, skip connections, layer depth, and convolutions. These features help to extract unimaginable features that contribute to reaching high recognition rates throughout the training of the network. Such

recognition architecture must be assigned as the mainly efficient, accurate, errorless, reliable, and flexible models for image partitioning to classify clinical lesion skin image applications.

REFERENCES

- [1] K. G. Paulson *et al.*, “Age-specific incidence of melanoma in the United States,” *JAMA Dermatology*, vol. 156, no. 1, Jan. 2020, doi: 10.1001/jamadermatol.2019.3353.
- [2] K. G. Lewis and M. A. Weinstock, “Trends in nonmelanoma skin cancer mortality rates in the United States, 1969 through 2000,” *Journal of Investigative Dermatology*, vol. 127, no. 10, pp. 2323–2327, Oct. 2007, doi: 10.1038/sj.jid.5700897.
- [3] A. Esteva *et al.*, “Dermatologist-level classification of skin cancer with deep neural networks,” *Nature*, vol. 542, no. 7639, pp. 115–118, Feb. 2017, doi: 10.1038/nature21056.
- [4] M. N. Bajwa *et al.*, “Computer-aided diagnosis of skin diseases using deep neural networks,” *Applied Sciences*, vol. 10, no. 7, Apr. 2020, doi: 10.3390/app10072488.
- [5] R. Zell *et al.*, “ICTV virus taxonomy profile: picornaviridae,” *Journal of General Virology*, vol. 98, no. 10, pp. 2421–2422, Oct. 2017, doi: 10.1099/jgv.0.000911.
- [6] S. W. Kashem, M. Haniffa, and D. H. Kaplan, “Antigen-presenting cells in the skin,” *Annual Review of Immunology*, vol. 35, no. 1, pp. 469–499, Apr. 2017, doi: 10.1146/annurev-immunol-051116-052215.
- [7] R. H. Abiyev and A. Helwan, “Fuzzy neural networks for identification of breast cancer using images’ shape and texture features,” *Journal of Medical Imaging and Health Informatics*, vol. 8, no. 4, pp. 817–825, May 2018, doi: 10.1166/jmihi.2018.2308.
- [8] Z. Xian, X. Wang, S. Yan, D. Yang, J. Chen, and C. Peng, “Main coronary vessel segmentation using deep learning in smart medical,” *Mathematical Problems in Engineering*, pp. 1–9, Oct. 2020, doi: 10.1155/2020/8858344.
- [9] B. N. Walker *et al.*, “Dermoscopy diagnosis of cancerous lesions utilizing dual deep learning algorithms via visual and audio (sonification) outputs: Laboratory and prospective observational studies,” *EBioMedicine*, vol. 40, pp. 176–183, Feb. 2019, doi: 10.1016/j.ebiom.2019.01.028.
- [10] A. Hekler *et al.*, “Effects of label noise on deep learning-based skin cancer classification,” *Frontiers in Medicine*, vol. 7, May 2020, doi: 10.3389/fmed.2020.00177.
- [11] K. Sriwong, S. Bunrit, K. Kerdprasop, and N. Kerdprasop, “Dermatological classification using deep learning of skin image and patient background knowledge,” *International Journal of Machine Learning and Computing*, vol. 9, no. 6, pp. 862–867, Dec. 2019, doi: 10.18178/ijmlc.2019.9.6.884.
- [12] M. C. M. Zon, J. D. Waa, M. Veta, and G. A. M. Krekels, “Whole-slide margin control through deep learning in Mohs micrographic surgery for basal cell carcinoma,” *Experimental Dermatology*, vol. 30, no. 5, pp. 733–738, May 2021, doi: 10.1111/exd.14306.
- [13] A. Rezvantalab, H. Safigholi, and S. Karimijeshni, “Dermatologist level dermoscopy skin cancer classification using different deep learning convolutional neural networks algorithms,” *arXiv preprint arXiv:1810.10348*, Oct. 2018.
- [14] O. T. Jones, C. K. I. Ranmuthu, P. N. Hall, G. Funston, and F. M. Walter, “Recognising skin cancer in primary care,” *Advances in Therapy*, vol. 37, no. 1, pp. 603–616, Jan. 2020, doi: 10.1007/s12325-019-01130-1.
- [15] S. S. Chaturvedi, J. V. Tembhurne, and T. Diwan, “A multi-class skin cancer classification using deep convolutional neural networks,” *Multimedia Tools and Applications*, vol. 79, no. 39–40, pp. 28477–28498, Oct. 2020, doi: 10.1007/s11042-020-09388-2.
- [16] H.-H. Wang, Y.-H. Wang, C.-W. Liang, and Y.-C. Li, “Assessment of deep learning using nonimaging information and sequential medical records to develop a prediction model for nonmelanoma skin cancer,” *JAMA Dermatology*, vol. 155, no. 11, Nov. 2019, doi: 10.1001/jamadermatol.2019.2335.
- [17] D. E. Webster *et al.*, “The mole mapper study, mobile phone skin imaging and melanoma risk data collected using ResearchKit,” *Scientific Data*, vol. 4, no. 1, Feb. 2017, doi: 10.1038/sdata.2017.5.
- [18] J. Deng, W. Dong, R. Socher, L.-J. Li, K. Li, and L. Fei-Fei, “ImageNet: A large-scale hierarchical image database,” in *2009 IEEE Conference on Computer Vision and Pattern Recognition*, Jun. 2009, pp. 248–255. doi: 10.1109/CVPR.2009.5206848.
- [19] M. Jaderberg, “Deep learning for text spotting,” PhD Thesis, University of Oxford, 2015.
- [20] N. A. Tu, T. Huynh-The, K.-S. Wong, D.-M. Bui, and Y.-K. Lee, “Distributed feature extraction on apache spark for human action recognition,” in *2020 14th International Conference on Ubiquitous Information Management and Communication (IMCOM)*, Jan. 2020, pp. 1–6. doi: 10.1109/IMCOM48794.2020.9001680.
- [21] O. Russakovsky *et al.*, “ImageNet large scale visual recognition challenge,” *International Journal of Computer Vision*, vol. 115, no. 3, pp. 211–252, Dec. 2015, doi: 10.1007/s11263-015-0816-y.
- [22] H. Kim, S. Lee, and H. Jung, “Human activity recognition by using convolutional neural network,” *International Journal of Electrical and Computer Engineering (IJECE)*, vol. 9, no. 6, pp. 5270–5276, Dec. 2019, doi: 10.11591/ijece.v9i6.pp5270-5276.
- [23] D. Silver *et al.*, “Mastering the game of Go with deep neural networks and tree search,” *Nature*, vol. 529, no. 7587, pp. 484–489, Jan. 2016, doi: 10.1038/nature16961.
- [24] J. R. Hagerty *et al.*, “Deep learning and handcrafted method fusion: higher diagnostic accuracy for melanoma dermoscopy images,” *IEEE Journal of Biomedical and Health Informatics*, vol. 23, no. 4, pp. 1385–1391, Jul. 2019, doi: 10.1109/JBHI.2019.2891049.
- [25] UNICAMP, “Robust melanoma screening-datasets,” Robust Melanoma Screening project. Accessed: Apr. 10, 2021. [Online]. Available: <https://sites.google.com/site/robustmelanomascreeing/dataset>
- [26] V. Sharma and N. Singh, “Deep convolutional neural network with ResNet-50 learning algorithm for copy-move forgery detection,” in *2021 7th International Conference on Signal Processing and Communication (ICSC)*, Nov. 2021, pp. 146–150. doi: 10.1109/ICSC53193.2021.9673422.
- [27] K. Weiss, T. M. Khoshgoftar, and D. Wang, “A survey of transfer learning,” *Journal of Big Data*, vol. 3, no. 1, Dec. 2016, doi: 10.1186/s40537-016-0043-6.
- [28] K. He, X. Zhang, S. Ren, and J. Sun, “Deep residual learning for image recognition,” in *2016 IEEE Conference on Computer Vision and Pattern Recognition (CVPR)*, Jun. 2016, pp. 770–778. doi: 10.1109/CVPR.2016.90.
- [29] S. Almadby and L. Elrefaei, “Deep convolutional neural network-based approaches for face recognition,” *Applied Sciences*, vol. 9, no. 20, Oct. 2019, doi: 10.3390/app9204397.
- [30] M. T. Hagos and S. Kant, “Transfer learning based detection of diabetic retinopathy from small dataset,” *arXiv preprint arXiv:1905.07203*, May 2019.

- [31] H. Zhu, H. Wei, B. Li, X. Yuan, and N. Kehtarnavaz, "A review of video object detection: datasets, metrics and methods," *Applied Sciences*, vol. 10, no. 21, Nov. 2020, doi: 10.3390/app10217834.
- [32] M. Emad and A. R. Ajel, "Auto analysis of defibrillation process based on wavelet transform," *IOP Conference Series: Materials Science and Engineering*, vol. 745, no. 1, Mar. 2020, doi: 10.1088/1757-899X/745/1/012095.
- [33] P. Patel and A. Thakkar, "The upsurge of deep learning for computer vision applications," *International Journal of Electrical and Computer Engineering (IJECE)*, vol. 10, no. 1, pp. 538–548, Feb. 2020, doi: 10.11591/ijece.v10i1.pp538-548.
- [34] M. Hammad, M. Al-Smadi, Q. B. Baker, and S. A. Al-Zboon, "Using deep learning models for learning semantic text similarity of Arabic questions," *International Journal of Electrical and Computer Engineering (IJECE)*, vol. 11, no. 4, Aug. 2021, doi: 10.11591/ijece.v11i4.pp3519-3528.
- [35] F. F. Alkhalid, A. Q. Albayati, and A. A. Alhammad, "Expansion dataset COVID-19 chest X-ray using data augmentation and histogram equalization," *International Journal of Electrical and Computer Engineering*, vol. 12, no. 2, pp. 1904–1909, 2022, doi: 10.11591/ijece.v12i2.pp1904-1909.
- [36] A. S. Narasimha Raju, K. Jayavel, and T. Rajalakshmi, "Intelligent recognition of colorectal cancer combining application of computer-assisted diagnosis with deep learning approaches," *International Journal of Electrical and Computer Engineering (IJECE)*, vol. 12, no. 1, pp. 738–747, Feb. 2022, doi: 10.11591/ijece.v12i1.pp738-747.
- [37] R. Saifan and F. Jubair, "Six skin diseases classification using deep convolutional neural network," *International Journal of Electrical and Computer Engineering (IJECE)*, vol. 12, no. 3, pp. 3072–3082, Jun. 2022, doi: 10.11591/ijece.v12i3.pp3072-3082.
- [38] T. S. Lim, K. G. Tay, A. Huong, and X. Y. Lim, "Breast cancer diagnosis system using hybrid support vector machine-artificial neural network," *International Journal of Electrical and Computer Engineering (IJECE)*, vol. 11, no. 4, pp. 3059–3069, Aug. 2021, doi: 10.11591/ijece.v11i4.pp3059-3069.
- [39] A. R. Nasser *et al.*, "IoT and cloud computing in health-care: a new wearable device and cloud-based deep learning algorithm for monitoring of diabetes," *Electronics*, vol. 10, no. 21, Nov. 2021, doi: 10.3390/electronics10212719.
- [40] J. Abdulhadi, A. Al-Dujaili, A. J. Humaidi, and M. A.-R. Fadhel, "Human nail diseases classification based on transfer learning," *ICIC Express Letters*, vol. 15, no. 12, pp. 1271–1282, 2021.
- [41] M. Q. Kasim, R. F. Hassan, A. J. Humaidi, A. I. Abdulkareem, A. R. Nasser, and A. Alkhayyat, "Control algorithm of five-level asymmetric stacked converter based on xilinx system generator," in *2021 IEEE 9th Conference on Systems, Process and Control (ICSPC 2021)*, Dec. 2021, pp. 174–179. doi: 10.1109/ICSPC53359.2021.9689173.
- [42] A. J. Humaidi, M. A. Fadhel, and A. R. Ajel, "Lane detection system for day vision using altera DE2," *TELKOMNIKA (Telecommunication Computing Electronics and Control)*, vol. 17, no. 1, pp. 349–361, Feb. 2019, doi: 10.12928/telkomnika.v17i1.10071.
- [43] A. J. Humaidi, T. M. Kadhim, S. Hasan, I. Kasim Ibraheem, and A. Taher Azar, "A generic izhikevich-modelled FPGA-realized architecture: a case study of printed English letter recognition," in *2020 24th International Conference on System Theory, Control and Computing (ICSTCC)*, Oct. 2020, pp. 825–830. doi: 10.1109/ICSTCC50638.2020.9259707.
- [44] A. J. Humaidi and T. M. Kadhim, "Spiking versus traditional neural networks for character recognition on FPGA platform," *Journal of Telecommunication, Electronic and Computer Engineering (JTEC)*, vol. 10, no. 3, pp. 109–115, 2018.
- [45] S. Nasir, M. Croock, and S. Al-Qaraawi, "Software engineering based fault tolerance model for information system in plants shopping center," *International Journal of Electrical and Computer Engineering*, vol. 10, no. 6, pp. 6664–6672, 2020, doi: 10.11591/IJECE.V10I6.PP6664-6672.
- [46] F. F. Shero, G. T. S. Al-Ani, E. J. Khadim, and H. ZuhairKhaleel, "Assessment of linear parameters of Electrohysterograph (EHG) in diagnosis of true labor," *Annals of Tropical Medicine and Public Health*, vol. 23, no. 4, 2020, doi: 10.36295/ASRO.2020.23418.
- [47] R. F. Hassan, A. R. Ajel, S. J. Abbas, and A. J. Humaidi, "FPGA based HIL co-simulation of 2DOF-PID controller tuned by PSO optimization algorithm," *ICIC Express Letters*, vol. 16, no. 12, pp. 1269–1278, 2022.
- [48] T. Ghanim, A. R. Ajel, and A. j. Humaidi, "Optimal fuzzy logic control for temperature control based on social spider optimization," *IOP Conference Series: Materials Science and Engineering*, vol. 745, no. 1, Mar. 2020, doi: 10.1088/1757-899X/745/1/012099.
- [49] A. J. Humaidi and M. R. Hameed, "Design and performance investigation of block-backstepping algorithms for ball and arc system," in *2017 IEEE International Conference on Power, Control, Signals and Instrumentation Engineering (ICPCSI)*, Sep. 2017, pp. 325–332. doi: 10.1109/ICPCSI.2017.8392309.
- [50] A. J. Humaidi, A. H. Hameed, and M. R. Hameed, "Robust adaptive speed control for DC motor using novel weighted E-modified MRAC," in *2017 IEEE International Conference on Power, Control, Signals and Instrumentation Engineering (ICPCSI)*, Sep. 2017, pp. 313–319. doi: 10.1109/ICPCSI.2017.8392302.
- [51] A. J. Humaidi, S. K. Kadhim, M. E. Sadiq, S. J. Abbas, A. Q. Al-Dujaili, and A. R. Ajel, "Design of optimal sliding mode control of pam-actuated hanging mass," *ICIC Express Letters*, vol. 16, no. 11, pp. 1193–1204, 2022.
- [52] A. R. Ajel, H. M. Abdul Abbas, and M. J. Mnati, "Position and speed optimization of servo motor control through FPGA," *International Journal of Electrical and Computer Engineering (IJECE)*, vol. 11, no. 1, pp. 319–327, Feb. 2021, doi: 10.11591/ijece.v11i1.pp319-327.

BIOGRAPHIES OF AUTHORS



Ahmed R. Ajel    was born in Iraq Baghdad. He received education of B.Sc., M.Sc. and Ph.D. In Electrical and Electronics Engineering in 1992, 1997, and 2006 respectively in University of Technology, in Electrical and Electronics Engineering Department. He can be contacted at email: dr_ahmed.r@mtu.edu.iq.



Ayad Qasim Al-Dujaili    is a lecturer in the Electrical Engineering Technical College/Middle Technical University, Baghdad, Iraq. He received the B.Sc. and M.Sc. degrees in Electrical and Electronics Engineering/Control from the University of Technology, Baghdad, Iraq, in 1992 and 2003, respectively. He received his Ph.D. degree in Control and Automation from the University of Lille, Lille, France in 2018. His current research interests include advanced control, intelligent control, nonlinear systems, robotics. He can be contacted at email: ayad.qasim@mtu.edu.iq.



Zaid G. Hadi    has attained the B.Sc. from Department of Medical Instrumentation/Electrical Engineering Technical College/Middle Technical University. He has been awarded the Degree of M.Sc. in the specialization of medical instrumentation from Electrical Engineering Technical College in 2022. He can be contacted at email: zaidghazi2020@gmail.com.



Amjad Jaleel Humaidi    received his B.Sc. and M. Sc. degrees in Control Engineering from Al-Rasheed College of Engineering and Science the University of Technology, Baghdad, Iraq, in 1992 and 1997, respectively. He received his Ph.D. degree from the University of Technology in 2006 with specialization of control and automation. He is presently a staff member of Control and System Engineering Department at University of Technology-Iraq. His fields of interest include advanced control (adaptive control, backstepping control, nonlinear optimal control, nonlinear observers, and active rejection control), intelligent control, optimization and identification. He can be contacted at email: amjad.j.humaidi@uotechnology.edu.iq.